α decay of the very neutron-deficient isotopes $^{197-199}$Fr

Z. Kalaninová,[1,*] A. N. Andreyev,[2,3,4] S. Antalic,[1] F. P. Heßberger,[5,6] D. Ackermann,[5] B. Andel,[1] M. C. Drummond,[7] S. Hofmann,[5] M. Huyse,[8] B. Kindler,[5] J. F. W. Lane,[2] V. Liberati,[2] B. Lommel,[5] R. D. Page,[7] E. Rapisarda,[8] K. Sandhu,[2] Š. Šáro,[1] A. Thornthwaite,[7] and P. Van Duppen[8]

[1]*Department of Nuclear Physics and Biophysics, Comenius University, 842 48 Bratislava, Slovakia*
[2]*University of the West of Scotland, Paisley PA1 2BE, United Kingdom*
[3]*Department of Physics, University of York, York YO10 5DD, United Kingdom*
[4]*Advanced Science Research Center (ASRC), Japan Atomic Energy Agency (JAEA), Tokai-mura, Ibaraki 319-1195, Japan*
[5]*GSI Helmholtzzentrum für Schwerionenforschung GmbH, 64291 Darmstadt, Germany*
[6]*Helmholtz Institut Mainz, 55099 Mainz, Germany*
[7]*Department of Physics, Oliver Lodge Laboratory, University of Liverpool, Liverpool L69 7ZE, United Kingdom*
[8]*Instituut voor Kern- en Stralingsfysica, K.U. Leuven, 3001 Leuven, Belgium*

(Received 29 January 2013; published 29 April 2013)

Decay properties of the very neutron-deficient isotopes $^{197-199}$Fr were studied at the velocity filter Separator for Heavy Ion reaction Products (SHIP) at GSI in Darmstadt. The isotopes were produced in the $2n$–$4n$ evaporation channels of the fusion-evaporation reaction $^{60}\mathrm{Ni} + ^{141}\mathrm{Pr} \rightarrow ^{201}\mathrm{Fr}^*$. Improved α-decay properties of ^{199}Fr were determined and the possible existence of two α-decaying states in this nucleus is discussed. For the isotope ^{198}Fr a broad α-decay energy distribution was detected in the range of (7470–7930) keV and two α-decaying states were observed with half-lives of 1.1(7) and 15(3) ms. The new isotope ^{197}Fr was identified based on the observation of one α-decay chain yielding $E_\alpha = 7728(15)$ keV and $T_{1/2} = 0.6^{+3.0}_{-0.3}$ ms. The systematics of reduced α-decay widths are presented for neutron-deficient francium, radon, and astatine isotopes.

DOI: 10.1103/PhysRevC.87.044335 PACS number(s): 23.60.+e, 21.10.Tg, 27.80.+w

I. INTRODUCTION

The region of neutron-deficient nuclei around lead provides a possibility to study several interesting nuclear-structure phenomena, e.g., shape coexistence and the sudden changes in deformation between neighboring nuclei (see, e.g., Refs. [1–4]). The investigation of nuclei in this region requires sensitive experimental methods due to low production cross sections and short half-lives. One of these methods that is applicable to neutron-deficient nuclei in the vicinity of the $Z = 82$ shell closure is α-decay spectroscopy.

Information on excited levels in the lightest neutron-deficient odd-A francium ($Z = 87$) isotopes is presently very scarce. As expected from a simple shell-model description, in most of these francium isotopes the spin and parity of the ground state is $9/2^-$, presumably related to a $\pi(h_{9/2})^5$ configuration. However, a proton intruder state with a $\pi(s_{1/2})^{-1}$ configuration, due to a proton excitation across the $Z = 82$ shell gap, was recently proposed to exist at low excitation energy in ^{201,203}Fr [5].

The lightest francium isotope isotope for which results had been published prior to the present study is ^{199}Fr. It was observed for the first time in the $6n$ evaporation channel of the fusion-evaporation reaction $^{36}\mathrm{Ar} + ^{169}\mathrm{Tm} \rightarrow ^{205}\mathrm{Fr}^*$ at the Gas-filled Recoil Ion Separator (GARIS) separator at The Institute of Physical and Chemical Research (RIKEN) [6]. Five α-decay chains were attributed to the decay of ^{199}Fr on the basis of correlations with the known α decay of the daughter isotope ^{195}At. The decay properties of ^{199}Fr were determined as $E_\alpha = 7655(40)$ keV and $T_{1/2} = 12^{+10}_{-4}$ ms. Recently, an α-decay study of ^{198,199}Fr was performed at the gas-filled separator Recoil Ion Transport Unit (RITU) at The University of Jyväskylä (JYFL) [7]. However, to our knowledge, no results were published so far.

In this paper we report on a detailed α-decay study of ^{199}Fr, ^{198}Fr, and the identification of ^{197}Fr. The goal of this work was to explore the α-decay properties of these isotopes and to search for proton emission from them.

II. EXPERIMENT

We produced the $^{197-199}$Fr isotopes at GSI in Darmstadt applying the fusion-evaporation reaction $^{60}\mathrm{Ni} + ^{141}\mathrm{Pr} \rightarrow ^{201}\mathrm{Fr}^*$. The irradiations were performed at several beam energies in the range of (262–300) MeV in front of the target to cover the maximum cross sections for the $2n$–$4n$ evaporation channels. The beam of average intensity ~400 pnA (1 pnA = 6.242×10^9 particles/s) was provided by the UNIversal Linear ACcelerator (UNILAC).

The average thickness of the targets prepared from the $^{141}\mathrm{PrF_3}$ material was ~520 μg/cm^2, which is equivalent to a contribution of ~370 μg/cm^2 of ^{141}Pr. The target material was evaporated on a 40-μg/cm^2 carbon backing and covered with a ~10-μg/cm^2 carbon layer to avoid sputtering of the target material and to increase its emissivity. The target foils were mounted on a wheel rotating synchronously with the beam macro structure (5-ms long pulses at 50-Hz repetition frequency).

The products of fusion-evaporation reactions were separated from products of other reactions and from primary beam

*zdenka.kalaninova@fmph.uniba.sk

particles by the velocity filter Separator for Heavy Ion reaction Products (SHIP) [8]. The transmission of SHIP was estimated to be 40%. After separation, the evaporation residues (ERs) were implanted into a 300-μm thick 16-strip position-sensitive silicon detector (PSSD) [9]. According to GEANT 4 simulations [10] the efficiency of the PSSD was about 55% for the detection of full-energy α particles. The energy resolution for single strips of the PSSD was ~(30–35) keV (FWHM). The energy calibration of the PSSD was performed using the nuclides ^{191}Bi [6311(5) keV], ^{196}Po[6520(3) keV], ^{195}Po^{g} [6609(5) keV], ^{194}Po [6843(3) keV], and ^{197}At^{g} [6958(5) keV] [11] produced in the considered reaction. To detect α particles that escaped from the PSSD in the backward direction, a system of six silicon detectors (denoted as "BOX" in the following text) divided into 28 segments was placed upstream of the PSSD. The geometrical efficiency of the BOX system was 80% of 2π [12]. The energy resolution for the α particles measured by the PSSD + BOX system was ~70 keV (FWHM).

Two time-of-flight (TOF) detectors were installed in front of the PSSD [13]. The (anti)coincidence condition between the signals from the PSSD and the TOF system allowed decay events to be distinguished from implantation events. By measuring the TOF and the kinetic energy of implanted events, complete-fusion reaction products were distinguished from other implanted particles, such as scattered projectiles or transfer-reaction products.

For the detection of γ rays a germanium clover detector composed of four crystals placed closely behind the PSSD was used. Gamma rays were registered either as individual events or in coincidence with signals from the PSSD within a time window of 5 μs. The low-energy threshold for the germanium detector was ~35 keV. For the calibration of the germanium detector ^{133}Ba and ^{152}Eu sources were used. The detection efficiency for γ rays at ~80 keV was ~10 % [14].

The identification of the isotopes was based on the time and position correlations of implanted ERs and their subsequent α decays. For more details on the correlation method see Ref. [15]. The position difference between an ER and the following α decay (ER-α1 correlations) and between two α decays (α1-α2 correlations) was required to be within ±0.5 mm. The time windows Δt(ER-α1) and Δt(α1-α2) were selected as a compromise between minimizing random correlations and covering most of the true correlations.

III. EXPERIMENTAL RESULTS

A. Isotope ^{199}Fr

The data for the isotope ^{199}Fr were collected at several beam energies in the range of (262–272) MeV in front of the target. The energy interval was chosen to cover the maximum of the $2n$ evaporation channel according to calculations performed using the statistical model code HIVAP [16]. At these energies we did not expect a notable contribution from ^{198}Fr produced in the $3n$ evaporation channel.

The part of the α-decay spectrum from 6400 to 8000 keV measured in the PSSD in anticoincidence with the TOF system is presented in Fig. 1(a). The spectrum is dominated by the decays of Po and Rn isotopes produced in the αpxn and pxn evaporation channels, respectively. The measured α-decay energies of these isotopes are in agreement with the reference values [11] within 4 keV. No distinct α peaks with $E_\alpha > 7500$ keV were observed due to the background. Using a time window Δt(ER-α1) < 60 ms for position-correlated events, the background and longer-lived activities are strongly reduced, while a peak with $E_\alpha \approx 7675$ keV becomes visible [Fig. 1(b)]. The spectrum of parent-daughter α1-α2 correlations shown in Fig. 1(c) was obtained using a time window $\Delta t(\alpha 1\text{-}\alpha 2) < 1.5$ s. The dominant groups in this spectrum are Rn (α1)-Po (α2) correlations. Three groups of α2 decays were observed in correlation with the α1 decay at 7675 keV. In Fig. 1(c) these groups are marked as A (4 full-energy events in the PSSD for both α1 and α2), B (26 events), and C (6 events). By considering the escaped events measured by the PSSD + BOX system, the total number of observed events in regions A, B, and C increases to 58.

The measured decay properties $E_{\alpha 2} = 6955(8)$ keV and $T_{1/2} = 350^{+240}_{-100}$ ms, for the α2 decay in region A of Fig. 1(c) are in a good agreement with the reported values for the α decay of ^{195}At^{g} ($E_\alpha = 6953(3)$ keV, $T_{1/2} = 328(20)$ ms [17]). Therefore we assign the parent α1 decay for region A with $E_{\alpha 1} = 7664(11)$ keV and $T_{1/2} = 4.5^{+3.1}_{-1.3}$ ms to ^{199}Fr.

The measured half-lives of 120^{+25}_{-20} ms and 130^{+70}_{-40} ms for the α2 decay of the groups B and C, respectively, correspond to the half-life of ^{195}At^{m} ($T_{1/2} = 147(5)$ ms [17]). The measured energy range of (7040–7200) keV for α2 decays from region B and $E_{\alpha 2} = 7248(6)$ keV for region C are also in line with the values for α decay of ^{195}At^{m} (see Fig. 7). Therefore we assign the parent α1 decay for events in regions B and C with $E_{\alpha 1} = 7676(6)$ keV and $T_{1/2} = 6.2^{+1.1}_{-0.8}$ ms to ^{199}Fr.

The small differences in half-lives and α-decay energies for α1 transitions at 7664(11) keV (region A) and 7676(6) keV (regions B and C) may indicate the presence of two different isomeric states in ^{199}Fr decaying to two isomeric states in ^{195}At. However, this difference could also be due to low statistics and limited energy resolution of the PSSD. This would suggest the presence of only one α-decaying state in ^{199}Fr with $E_\alpha = 7675(6)$ keV and $T_{1/2} = 6.0^{+1.0}_{-0.7}$ ms. We present the discussion of both scenarios in Sec. IV A.

The α-decay energy and half-life for ^{199}Fr obtained from our data are in line with the values of $E_\alpha = 7655(40)$ keV and $T_{1/2} = 12^{+10}_{-4}$ ms reported previously [6], but have higher precision. At the beam energy of 267 MeV we deduced the maximum cross section of 3.1(13) nb for ^{199}Fr production.

B. Isotope ^{198}Fr

The data for the isotope ^{198}Fr were collected at several beam energies in the range of (282–300) MeV in front of the target. The energy range was chosen to cover the maximum of the $3n$ evaporation channel and to minimize the contribution from the $2n$ evaporation channel.

The part of the α-decay spectrum from 6400 to 8000 keV measured in the PSSD in anticoincidence with the TOF system is shown in Fig. 2(a). The dominant α lines belong to Po isotopes produced in the αpxn evaporation channels and astatine isotopes produced in the $2pxn$ or αxn evaporation

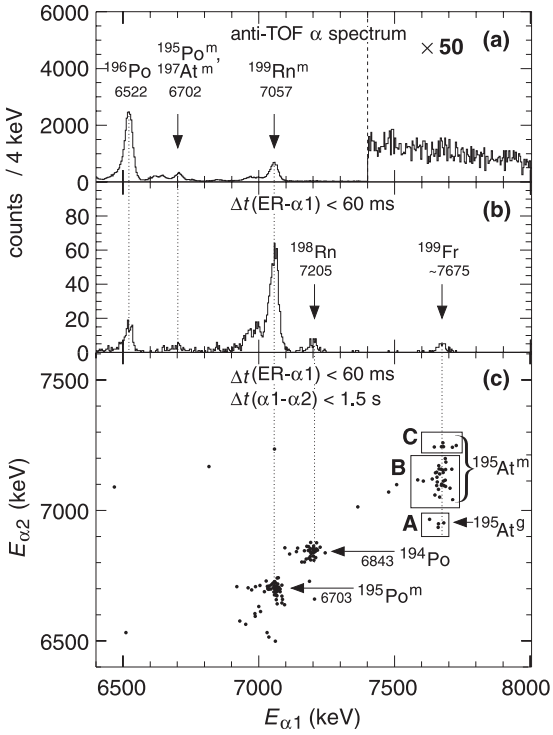

FIG. 1. (a) The sum of α-decay energy spectra measured in the PSSD in anticoincidence with the TOF detectors in the reaction $^{60}\mathrm{Ni} + ^{141}\mathrm{Pr}$ at several beam energies in the range of (262–272) MeV. (b) α decays from (a) detected within 60 ms after an ER implantation. (c) Parent-daughter α1-α2 correlation spectrum. α2 decays were detected within 1.5 s after α1 decays from (b).

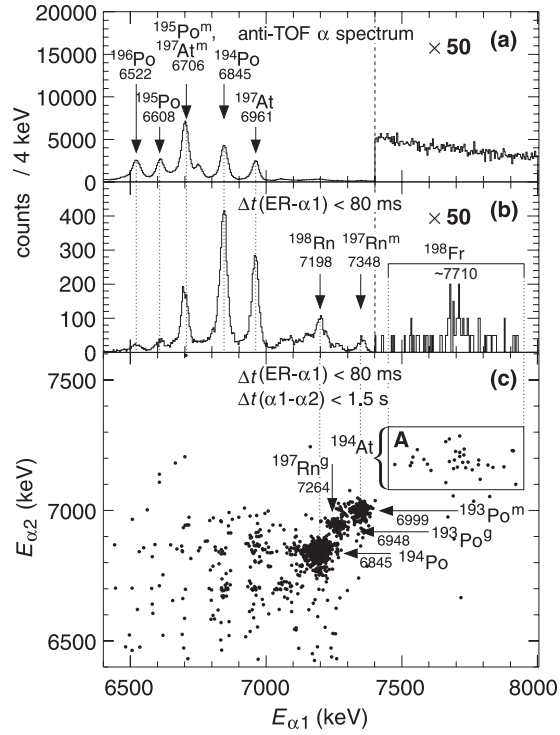

FIG. 2. (a) The sum of α-decay energy spectra measured in the PSSD in anticoincidence with the TOF detectors in the reaction $^{60}\mathrm{Ni} + ^{141}\mathrm{Pr}$ at several beam energies in the range of (282–300) MeV. (b) α decays from (a) detected within 80 ms after an ER implantation. (c) Parent-daughter α1-α2 correlation spectrum. α2 decays were detected within 1.5 s after α1 decays from (b).

channels. Within 80 ms after ER implantations, α1 decays with a broad energy distribution in the range of (7470–7930) keV were detected [see Fig. 2(b)]. The spectrum of parent-daughter α1-α2 correlations shown in Fig. 2(c) was obtained by applying the condition $\Delta t(\alpha 1\text{-}\alpha 2) < 1.5$ s. The dominant groups in this spectrum are decays of ^{198,197}Rn (α1) produced in the pxn evaporation channels correlated with their daughters ^{194,193}Po (α2).

The α1 decays in region A of Fig. 2(c) are correlated with an α2 activity with $T_{1/2} = 210^{+30}_{-20}$ ms. This value is in agreement with the half-life of 253(10) ms for $^{194}\mathrm{At}^{m1}$ and compatible within a 3-σ interval with the half-life of 310(8) ms for $^{194}\mathrm{At}^{m2}$ [18]. The measured energy distribution of α2 decays in the range of (7140–7290) keV agrees with values for both $^{194}\mathrm{At}^{m1}$ and $^{194}\mathrm{At}^{m2}$ reported in Ref. [18], for which two main α lines were observed at 7178(15) and 7190(15) keV. Based on the ER-α1-α2 analysis, we attribute the parent decay in region A of Fig. 2(c) to the isotope ^{198}Fr. In total 72 ER-α1-α2 (^{198}Fr-^{194}At) correlation chains were detected including events with coincidence signals between the PSSD and BOX system; 37 events were registered with full-energy release in PSSD. Despite the overlapping α-decay energy regions of ^{198}Fr and ^{199}Fr, both isotopes can be clearly distinguished using the different beam energies for their production. For ^{199}Fr a single peak at 7675 keV was observed [see Fig. 3(a)] compared to the α-decay energy range of (7470–7930) keV for ^{198}Fr [see Fig. 3(b)].

The time distribution of ^{198}Fr decays can be explained by the presence of two components (see Fig. 4). The fit to the experimental decay curve was obtained with a combination of a shorter-lived component with $T_{1/2} = 1.1(7)$ ms and a longer-lived component with $T_{1/2} = 15(3)$ ms. Within the limited statistics the α-decay energy distribution of the shorter-lived state seems to be concentrated at energies higher than 7700 keV [see Fig. 3(c)]. In contrast to this, the α decay of the longer-lived state has a broader energy distribution in the range of (7470–7920) keV with an indication of a distinct α line at ~7710 keV [see Fig. 3(d)].

The granddaughter α3 decay was searched for within a 10-s correlation time after an α2 decay. The detected α3-decay energy was in the range of ~(6410–6475) keV corresponding to $^{190}\mathrm{Bi}^{m1,m2}$ (with reference values $E_\alpha = 6431(5)$ keV, $T_{1/2} = 6.3(1)$ s for $^{190}\mathrm{Bi}^{m1}$, and $E_\alpha = 6456(5)$ keV, $T_{1/2} = 6.2(1)$ s for $^{191}\mathrm{Bi}^{m2}$ [19,20]) (see Fig. 5). The lower number of α3 decays in Fig. 5 compared to the number of events in Fig. 2(c) (region A) is due to the α-decay branching ratio of ^{190}Bi ($b_\alpha = 90^{+10}_{-30}$% for $^{190}\mathrm{Bi}^{m1}$ and $b_\alpha = 70(9)$% for $^{190}\mathrm{Bi}^{m2}$ [19]) and the limited α2-α3 correlation time. The α3 decays also support the presence of two states in ^{198}Fr. The α1 decays with $\Delta t(\mathrm{ER}\text{-}\alpha 1) \leqslant 5$ ms correlate with the ~6415- and ~6460-keV decays from both $^{190}\mathrm{Bi}^{m1}$ and $^{190}\mathrm{Bi}^{m2}$ states [see Fig. 5(a)], while the α1 decays with $\Delta t(\mathrm{ER}\text{-}\alpha 1) > 5$ ms only correlate with the ~6425-keV decays of $^{190}\mathrm{Bi}^{m1}$ [(see Fig. 5(b)].

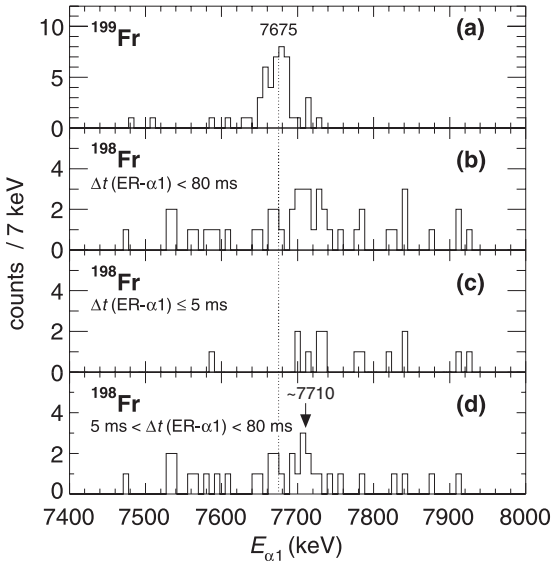

FIG. 3. (a) The part of the $\alpha 1$-decay spectrum of ^{199}Fr measured in the PSSD from Fig. 1(b) correlated with the $\alpha 2$ decays with the same search conditions as in Fig. 1(c), including escaped $\alpha 2$ events detected by the PSSD + BOX system. (b) Same as (a) but for ^{198}Fr decays from Fig. 2(b). (c) α decays from (b) occurring within 5 ms after ER implantation. (d) α decays from (b) occurring between 5 and 80 ms after ER implantation.

Searching for ER-($\alpha 1$-γ)-$\alpha 2$-$\alpha 3$ correlations, two photons with $E_\gamma = 81.5(7)$ keV were detected in coincidence with 7836(14)-keV $\alpha 1$ decays. The energy of these photons agrees with the energy of $K_{\alpha 1}$ x rays of astatine with $E_{K_{\alpha 1}} = 81.517$ keV [21]. The time differences between the implantations of ERs and the detection of the $\alpha 1$-γ coincidences were 3.3 and 4.7 ms. Although the $\alpha 2$ particle from one decay chain was only registered with part of its energy in the PSSD, the $\alpha 3$ particle was fully stopped in the PSSD for both decay chains. The energies of the $\alpha 3$ decays 6470(15) and 6461(15) keV are consistent with the 6456(5)-keV α decay of ^{190}Bi^{m2}.

At the beam energy of 282 MeV, a maximum production cross section of 1.0(2) nb was deduced for the sum of the two

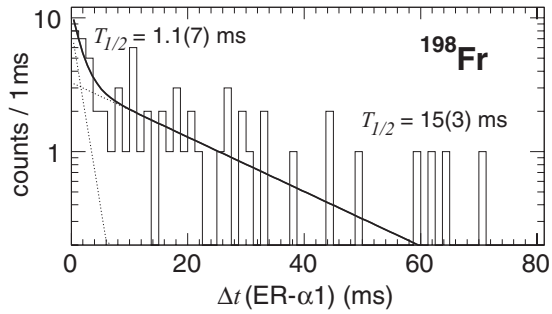

FIG. 4. The decay curve of ^{198}Fr [for the events from Fig. 3(b) including the escaped events detected by the PSSD + BOX system]. The fit function was obtained as a combination of two exponential components with half-lives of 1.1(7) and 15(3) ms depicted by dotted lines. The total decay curve as a sum of exponential components is drawn by a solid line.

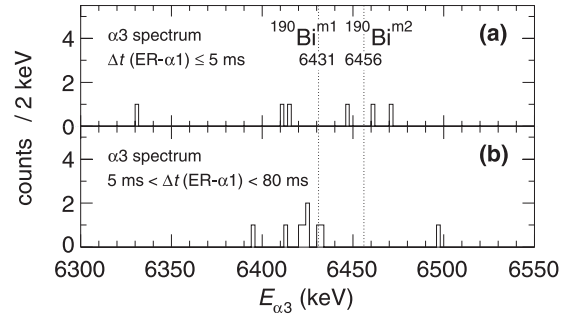

FIG. 5. The ^{198}Fr granddaughter $\alpha 3$-decay energy spectrum correlated with events from region A of Fig. 2(c) within 10 s. The dotted lines represent the reference energies [19] for ^{190}Bi^{m1,m2}. (a) $\alpha 3$ decays correlated with $\alpha 1$ decays of ^{198}Fr with $\Delta t(\text{ER-}\alpha 1) \leqslant 5$ ms. (b) $\alpha 3$ decays correlated with $\alpha 1$ decays of ^{198}Fr with 5 ms $< \Delta t(\text{ER-}\alpha 1) <$ 80 ms.

isomers in ^{198}Fr. From the total number of ^{198}Fr decays and their time distribution after ER implantations [see Figs. 3(c), 3(d), and 4] we estimate a population of 15(5)% for the shorter-lived state and 85(5)% for the longer-lived state.

C. New isotope ^{197}Fr

At the highest beam energy of 300 MeV, chosen specifically for the $4n$ evaporation channel, we observed one ER-$\alpha 1$-$\alpha 2$-$\alpha 3$ correlation chain with $\Delta t(\text{ER-}\alpha 1) = 0.9$ ms and $E_{\alpha 1} = 7728(15)$ keV (see Fig. 6). The $\alpha 1$ decay was followed by a 7375(30)-keV $\alpha 2$ decay after 45 ms. The granddaughter 6665(30)-keV $\alpha 3$ decay was detected 294 ms after the $\alpha 2$ decay. The $\alpha 1$ particle was fully stopped in the PSSD, while the $\alpha 2$ and $\alpha 3$ particles escaped from the PSSD, but their residual energies were registered by the BOX system.

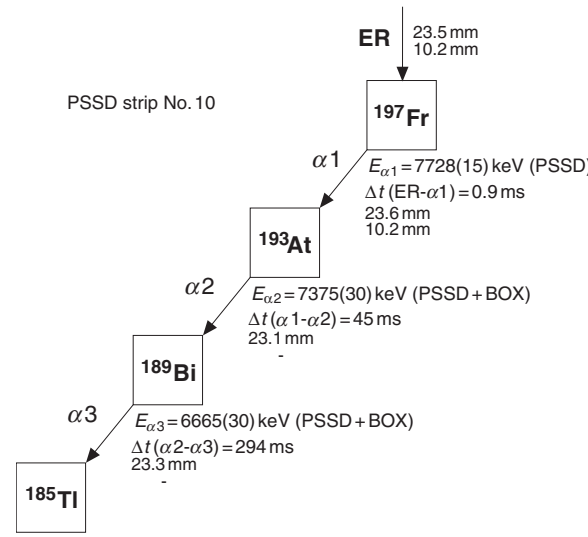

FIG. 6. Observed triple-α correlation decay chain attributed to ^{197}Fr. Measured energies, time differences between subsequent signals, and positions obtained from the top and bottom of the strip are shown. In the case of the escaped α particles $\alpha 2$ and $\alpha 3$, the signals from the bottom of the strip were too low for detection.

We associate the daughter α2 decay with the known α decay of ^{193}At ($E_\alpha = 7325(5)$ keV, $T_{1/2} = 21(5)$ ms [22]) and the granddaughter α3 decay with ^{189}Bi ($E_\alpha = 6667(4)$ keV, $T_{1/2} = 580(25)$ ms [22]). Therefore we attribute the parent 7728(15)-keV α1 decay with $T_{1/2} = 0.6^{+3.0}_{-0.3}$ ms to the new isotope ^{197}Fr. The probability of detecting such a triple-α correlation chain randomly, calculated using the method from Ref. [23], is 10^{-9}.

The production cross section of ^{197}Fr was determined as 18^{+41}_{-15} pb. A careful search for a possible proton-decay branch of ^{197}Fr was made by searching for ER-proton-α(^{196}Rn) correlations, but no evidence for this was found.

IV. DISCUSSION

A. Isotope ^{199}Fr

The ground states of odd-A francium isotopes from $A = 219$ down to $A = 201$ are presumed to have the configuration $\pi(h_{9/2})^5$ [11]. An α-decaying isomeric proton intruder $\pi(s_{1/2})^{-1}$ state was identified in ^{201}Fr [5]. Its excitation energy was estimated to be either 146 [5] or 129 keV [24] (without quoted uncertainties). In the heavier isotope ^{203}Fr, the presence of a $1/2^+$ level was also suggested, but its excitation energy was not reported [5]. The expected $\pi(f_{7/2})$ state was deduced to lie above the $1/2^+$ level in ^{201}Fr and below the $1/2^+$ level in ^{203}Fr [5]. As in the lightest odd-A astatine ($Z = 85$) and Bi ($Z = 83$) isotopes, all three of these levels ($9/2^-, 7/2^-, 1/2^+$) can also be expected to lie close in energy in ^{199}Fr. We note that all spins and parities in this paper are tentative.

Two α-decaying states are presently known in ^{195}At with assumed spins $7/2^-$ (isomeric state) and $1/2^+$ (ground state). Our data indicate that the α decay of ^{199}Fr with $E_\alpha \approx 7675$ keV is correlated with α decays from both ^{195}At^m and ^{195}At^g. We present two possible scenarios for this observation as our data do not allow to discriminate between them.

One possible interpretation illustrated in the left panel of Fig. 7 is that two α-decaying states exist in ^{199}Fr with similar decay characteristics: 12(5)% of the decays having $E_\alpha = 7664(11)$ keV and $T_{1/2} = 4.5^{+3.1}_{-1.3}$ ms populating ^{195}At^g [region A in Fig. 1(c)], and 88(5)% decays with $E_\alpha = 7676(6)$ keV and $T_{1/2} = 6.2^{+1.1}_{-0.8}$ ms populating ^{195}At^m [regions B and C in Fig. 1(c)]. Following this scenario, the reduced α-decay widths (δ^2_α) calculated using the Rasmussen prescription [25] assuming $\Delta L = 0$ for transitions populating ^{195}At^g and ^{195}At^m are 120^{+80}_{-40} and 81^{+15}_{-11} keV, respectively. These values are comparable with the reduced α-decay width of the heavier isotope ^{201}Fr [$\delta^2_\alpha = 75(8)$ keV]. The hindrance factors (HFs) for these transitions of $0.7^{+0.5}_{-0.2}$ and 1.1(2), respectively, were evaluated by comparing the δ^2_α of these transitions with those of neighboring even-even isotopes [$\delta^2_\alpha(^{198}\text{Rn}) = 111(6)$ keV, $\delta^2_\alpha(^{200}\text{Rn}) = 64^{+11}_{-3}$ keV]. The values of HFs indicate unhindered decays for both transitions. Therefore, the spin and parity of the α-decaying levels in ^{199}Fr should be the same as in the daughter ^{195}At. The relative intensities of the transitions [12(5)% for $E_\alpha = 7664$ keV and 88(5)% for $E_\alpha = 7676$ keV] agree with the expectation of the higher population of high-spin states in comparison with low-spin states in complete-fusion reactions. In this scenario, based on the 32(7)-keV excitation energy of ^{195}At^m [17], the level in ^{199}Fr decaying to ^{195}At^m lies 47(7) keV above the level decaying to ^{195}At^g. The estimated upper limit for the possible $E3$ internal-transition (IT) decay between $7/2^-$ and $1/2^+$ levels in ^{195}At is $B(E3) < 0.03$ Weisskopf units.

There is an alternative interpretation of the data, which is illustrated in the right panel of Fig. 7. As the energies of the α1 decays correlated with the α2 decays from ^{195}At^m and ^{195}At^g are comparable within their statistical uncertainty, they may represent the same α decay from only one α-decaying state in ^{199}Fr with $E_{\alpha 1} = 7675(6)$ keV. This transition populates an isomeric $7/2^-$ level in ^{195}At, which is required to have two decay modes in this scenario — α decay [$b_\alpha = 88(5)\%$] and deexcitation through an unobserved 32(7)-keV $E3$ IT decay to the ground state [$b_{IT} = 12(5)\%$]. The $B(E3)$ value for the $E3$ IT decay is $0.09^{+0.14}_{-0.05}$ W.u. in this scenario. A similar value of 0.09 W.u. was deduced for the $E3$ IT decay connecting the same levels $1/2^+$ and $7/2^-$ in ^{191}Bi, the α-decay daughter of ^{195}At [17]. The reduced α-decay width for the 7675(6)-keV transition is 85^{+15}_{-11} keV and the HF value is 1.0(2) indicating an unhindered decay. Therefore, in this scenario, we would assign a spin and parity of $7/2^-$ to the observed α-decaying state in ^{199}Fr.

To summarize, improved data for ^{199}Fr were obtained in our work, which can be interpreted in two possible ways (see the decay schemes in Fig. 7). No preference for either

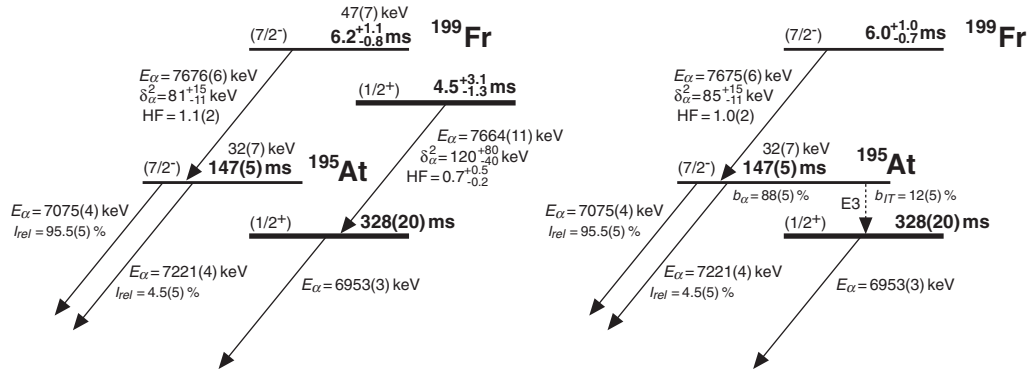

FIG. 7. Two possible α-decay schemes suggested for ^{199}Fr. The values for ^{199}Fr are from our measurement and for ^{195}At are from [17]. All spin and parity values are tentative.

of the scenarios can be expressed due to the relatively low statistics.

B. Isotope ^{198}Fr

In the even-A francium isotope ^{200}Fr only one α-decaying state has been observed so far [24], while in ^{202,204,206}Fr at least two α-decaying states have been identified [26]. In our data, the observation of two different half-lives [1.1(7) ms and 15(3) ms] and different energy distributions for the decay of ^{198}Fr [see Figs. 3(c) and 3(d)] implies two isomeric states also in this isotope. Furthermore, the $\alpha 1$ decay of ^{198}Fr with Δt(ER-$\alpha 1$) $>$ 5 ms is correlated only with $\alpha 3$ decays of ^{190}Bi^{m1} [see Fig. 5(b)], while the $\alpha 1$ decay with Δt(ER-$\alpha 1$) $\leqslant$ 5 ms seems to be followed by $\alpha 3$ decays from both ^{190}Bi^{m1} and ^{190}Bi^{m2} [see Fig. 5(a)]. However, the appearance of correlations with decays from ^{190}Bi^{m1} for $\alpha 1$ decaying with Δt(ER-$\alpha 1$) $\leqslant$ 5 ms is most probably due to the contribution of events from the 15(3)-ms state also present within 5 ms after ER implantation. Therefore, we assume that the shorter-lived state decays predominantly to ^{190}Bi^{m2} and the longer-lived state decays to ^{190}Bi^{m1} (see the proposed decay scheme in Fig. 8).

The broad α-decay energy distribution with a hint of a peak at $\sim$7710 keV for ^{198}Fr indicates its complex decay pattern [see Figs. 2(b), 2(c) (region A), and 3(b)]. For the 15(3)-ms state, if one assumes a relative intensity of $\sim$50 % for the $\sim$7710-keV α line [see Fig. 3(d)], then $\delta^2_\alpha \approx 10$ keV can be deduced. This suggests a hindrance of the $\sim$7710-keV transition relative to both ^{199}Fr [$\delta^2_\alpha = (81 - 120)$ keV] and neighboring even-even nuclei [$\delta^2_\alpha(^{196}\text{Rn}) = 250^{+80}_{-50}$ keV, $\delta^2_\alpha(^{198}\text{Rn}) = 111(6)$ keV, $\delta^2_\alpha(^{200}\text{Rn}) = 64^{+11}_{-3}$ keV]. This decay should populate an excited state at $\sim$210 keV in ^{194}At (see Fig. 8), as α decays from 15(3)-ms state have energies up to $\sim$7920 keV. We assume that this level deexcites partly through internal conversion, as we did not detect any $\sim$210-keV γ rays in coincidence with the α decays of ^{198}Fr. The energy summing of an α particle and conversion electrons can also explain the broad α-decay energy distribution of this state [see Fig. 3(d)]. However, the nonobservation of γ rays at $\sim$210 keV can also be explained by the low statistics and only $\sim$7.5% efficiency for the detection of γ rays with $E_\gamma \approx 200$ keV [14] or by the existence of other levels below the $\sim$210-keV state and then the deexcitation through a cascade of lower-energy transitions instead of one single transition. As there is a strong

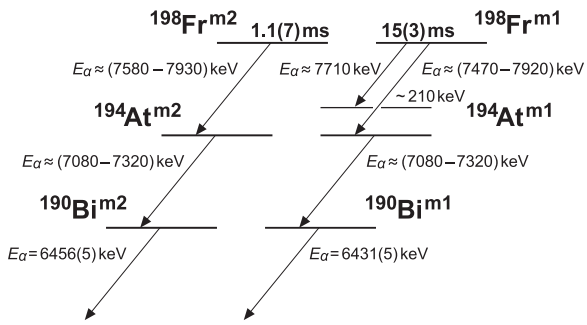

FIG. 8. Proposed simplified decay scheme for two states in ^{198}Fr. The relative positions of the isomeric states are not known.

contribution of α decays below 7710 keV, also at least one level above $\sim$210 keV must be populated by the α decay of ^{198}Fr.

We note that the Q_α value of 8078(7) keV for the highest-energy α transitions of ^{198}Fr [$E_\alpha = 7915(7)$ keV, see Fig. 3(b)] agrees with the value of 8093(14) keV, which is the sum of the Q_α value for the α decays detected in coincidence with the 81.5(7)-keV photons [$E_\alpha = 7836(14)$ keV] plus the K-binding energy of astatine ($E_B = 96$ keV [21]). However, the detected photons could also be γ-ray transitions that by chance have the same energy as $K_{\alpha 1}$ x rays of astatine. Based on the energies of correlated $\alpha 3$ decays corresponding to the decay of ^{190}Bi^{m2} and on the time differences between ERs and $\alpha 1$ decays (both within 5 ms), the $\alpha 1$-γ coincidences belong to the decay of ^{198}Fr^{m2}, but we omit placing them into the decay scheme as this would be too speculative.

In summary, the isotope ^{198}Fr was identified and an indication for two isomeric states was observed. Due to the complexity of the data and the low statistics only a simplified decay scheme is proposed (see Fig. 8).

C. Isotope ^{197}Fr

The reduced α-decay width for the α transition at 7728(15) keV attributed to the decay of ^{197}Fr is 600^{+2900}_{-300} keV. This suggests an HF of $0.3^{+1.5}_{-0.2}$ compared to neighboring even-even isotopes [$\delta^2_\alpha(^{194}\text{Rn}) = 270(60)$ keV, $\delta^2_\alpha(^{196}\text{Rn}) = 250^{+80}_{-50}$ keV, $\delta^2_\alpha(^{198}\text{Rn}) = 111(6)$ keV]. Although the uncertainty is large, the very low HF value indicates an allowed transition. Therefore, we assume no spin or parity change between the levels connected by this transition.

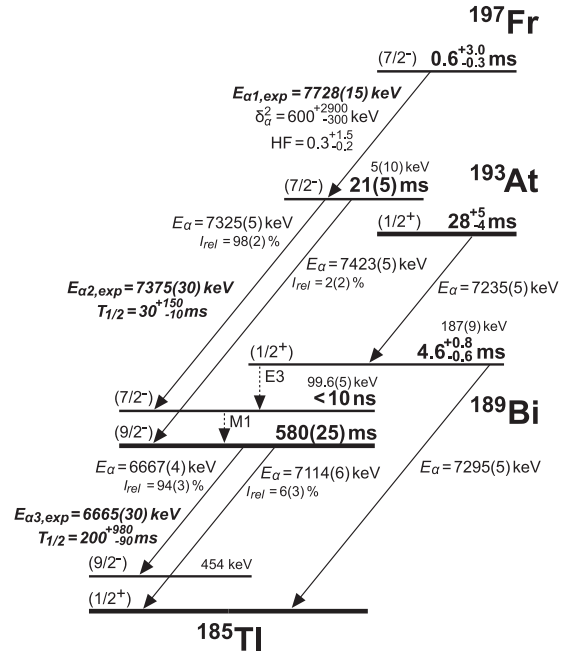

FIG. 9. The proposed decay scheme for ^{197}Fr. The reference values for decays of ^{193}At and ^{189}Bi are from Ref. [22]. The experimental values for $\alpha 1$, $\alpha 2$, and $\alpha 3$ decays from our measurement are written in bold italic font.

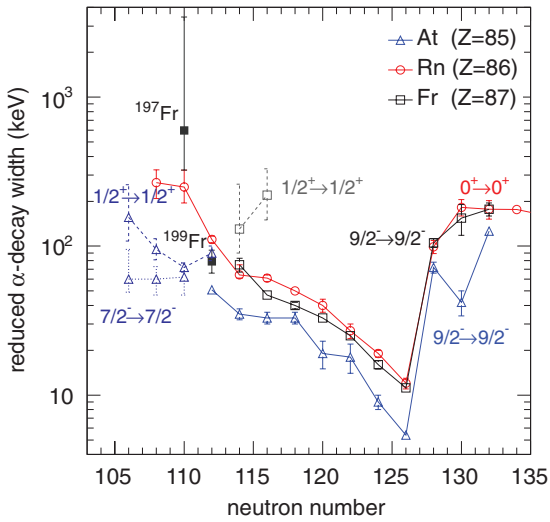

FIG. 10. (Color online) The systematics of reduced α-decay widths in the vicinity of the shell closure $N = 126$ for odd-A francium isotopes and neighboring odd-A astatine and even-A Rn isotopes. The $9/2^- \rightarrow 9/2^-$ and $0^+ \rightarrow 0^+$ transitions are connected by solid lines. The transitions $7/2^- \rightarrow 7/2^-$ and $1/2^+ \rightarrow 1/2^+$ are represented by dashed lines. The literature values are taken from Refs. [3,17,22,24,27–33]. The values from our measurement for ^{197,199}Fr are shown by solid symbols.

In ^{193}At, the $1/2^+$ and $7/2^-$ levels were observed to be very close in energy and it is presently not known unambiguously which one of them represents the ground state [22]. The energy and half-life for the $\alpha 2$ decay correlated with the parent ^{197}Fr decay agree with the α-decay properties of the $7/2^-$ state in ^{193}At (see Fig. 9). Therefore, we assume that the observed parent 7728(15)-keV α decay originates from the $7/2^-$ state in ^{197}Fr. This would also be in agreement with the expected higher population of higher-spin states compared with lower-spin states in complete-fusion reactions.

D. Systematics of reduced α-decay widths

The δ^2_α systematics for odd-A francium, astatine, and even-A Rn isotopes in the vicinity of the shell closure $N = 126$ are shown in Fig. 10. The francium isotopes exhibit an increasing trend of δ^2 with decreasing neutron number from $N = 126$ down to $N = 114$. The value of the reduced α-decay width for ^{199}Fr ($N = 112$) in the range of (81–120) keV (depending on the considered scenario, see Sec. IV A) obtained from our data indicates no significant change compared to ^{201}Fr. However, the deduced $\delta^2_\alpha(^{197}\text{Fr}) = 600^{+2900}_{-300}$ keV is considerably larger than in the heavier isotopes ^{199,201}Fr (see Fig. 10). Neighboring even-even Rn isotopes ($Z = 86$) have reduced α-decay widths of 270(60) keV (^{194}Rn) [30], 250^{+80}_{-50} keV (^{196}Rn) [31] and 111(6) keV (^{198}Rn) [3]. We note that the values of δ^2_α of the isotopes in this region (including ^{197}Fr) are higher than for transitions in regions above the doubly magic nuclei ^{100}Sn (e.g., $\delta^2_\alpha(^{105}\text{Te}) = 140(20)$ keV [34], $\delta^2_\alpha(^{106}\text{Te}) = 220^{+100}_{-80}$ keV [35,36]) or ^{208}Pb (e.g., $\delta^2_\alpha(^{212}\text{Po}) = 70(1)$ keV [11], $\delta^2_\alpha(^{213}\text{Po}) = 90(20)$ keV [11]). To investigate this issue more experimental data would be necessary.

V. CONCLUSION

In this work we present new α-decay data for very neutron-deficient francium nuclei. Significantly improved α-decay properties were obtained for ^{199}Fr compared to previously reported values [6]. We propose two possible scenarios for the decay of ^{199}Fr. One of them considers the existence of two α-decaying states with similar decay properties: the presumed $1/2^+$ state decaying to $^{195}\text{At}^g$ with $E_\alpha = 7664(11)$ keV, $T_{1/2} = 4.5^{+3.1}_{-1.3}$ ms and the presumed $7/2^-$ state decaying to $^{195}\text{At}^m$ with $E_\alpha = 7676(6)$ keV, $T_{1/2} = 6.2^{+1.1}_{-0.8}$ ms. The second scenario considers only one α-decaying state with tentative spin and parity $7/2^-$, $E_\alpha = 7675(6)$ keV, and $T_{1/2} = 6.0^{+1.0}_{-0.7}$ ms.

The isotope ^{198}Fr was identified with a broad α-decay energy distribution in the range (7470–7930) keV. The energy and time distribution of α decays as well as correlated granddaughter decays indicate the presence of two α-decaying states in ^{198}Fr with half-lives of 1.1(7) and 15(3) ms.

One ER-α-α-α correlation chain attributed to the new isotope ^{197}Fr was detected. This chain is assumed to originate from the $7/2^-$ level in ^{197}Fr. The obtained α-decay energy and half-life for ^{197}Fr are $E_\alpha = 7728(15)$ keV and $T_{1/2} = 0.6^{+3.0}_{-0.3}$ ms.

In addition, we present the systematics of reduced α-decay widths for the lightest odd-A francium, astatine, and even-A Rn isotopes.

ACKNOWLEDGMENTS

We thank the UNILAC staff for providing the stable and high intensity ^{60}Ni beam. This work was supported by FWO-Vlaanderen (Belgium), GOA/2004/03 (BOF-K.U.Leuven), IUAP — Belgian State Belgian Science Policy — (BriX network P7/12), European Community FP7 Capacities, Contract ENSAR No. 227867, UK Science and Technology Facilities Council (STFC), Slovak Research and Development Agency (Contract No. APVV-0105-10), Slovak grant agency VEGA (Contract No. 1/0576/13), Comenius University grant (Contract No. UK/218/2012), Reimei Foundation of Advanced Science Research Center (ASRC, JAEA), and DAIWA Anglo-Japanese Foundation.

[1] K. Heyde and J. L. Wood, Rev. Mod. Phys. **83**, 1467 (2011).
[2] A. N. Andreyev, M. Huyse, P. Van Duppen, L. Weissman, D. Ackermann, J. Gerl, F. P. Heßberger, S. Hofmann, A. Kleinböhl, G. Münzenberg, S. Reshitko, C. Schlegel, H. Schaffner, P. Cagarda, M. Matoš, Š. Šáro, A. Keenan, C. Moore, C. O'Leary, R. Page, M. Taylor, H. Kettunen, M. Leino, A. Lavrentiev, R. Wyss, and K. Heyde, Nature (London) **405**, 430 (2000).

[3] N. Bijnens, P. Decrock, S. Franchoo, M. Gaelens, M. Huyse, H.-Y. Hwang, I. Reusen, J. Szerypo, J. von Schwarzenberg, J. Wauters, J. G. Correia, A. Jokinen, P. Van Duppen, and The ISOLDE Collaboration, Phys. Rev. Lett. **75**, 4571 (1995).
[4] R. Julin, K. Helariutta, and M. Muikku, J. Phys. G: Nucl. Part. Phys. **27**, R109 (2001).
[5] J. Uusitalo, M. Leino, T. Enqvist, K. Eskola, T. Grahn, P. T. Greenlees, P. Jones, R. Julin, S. Juutinen, A. Keenan, H. Kettunen, H. Koivisto, P. Kuusiniemi, A.-P. Leppänen, P. Nieminen, J. Pakarinen, P. Rahkila, and C. Scholey, Phys. Rev. C **71**, 024306 (2005).
[6] Y. Tagaya, S. Hashimoto, K. Morita, Y. H. Pu, T. Ariga, K. Ohta, T. Minemura, I. Hisanaga, T. Motobayashi, and T. Nomura, Eur. Phys. J. A **5**, 123 (1999).
[7] J. Uusitalo (private communication).
[8] G. Münzenberg, W. Faust, S. Hofmann, P. Armbruster, K. Güttner, and H. Ewald, Nucl. Instrum. Methods **161**, 65 (1979).
[9] S. Hofmann and G. Münzenberg, Rev. Mod. Phys. **72**, 733 (2000).
[10] S. Agostinelli *et al.*, Nucl. Instrum. Methods **506**, 250 (2003); http://geant4.cern.ch/.
[11] R. B. Firestone and L. P. Ekström, database version 2/28/99 from URL http://ie.lbl.gov/toi/index.htm.
[12] A. N. Andreyev, D. Ackermann, F. P. Heßberger, S. Hofmann, M. Huyse, G. Münzenberg, R. D. Page, K. Van de Vel, and P. Van Duppen, Nucl. Instr. and Meth. A **533**, 409 (2004).
[13] Š. Šáro, R. Janik, S. Hofmann, H. Folger, F. P. Heßberger, V. Ninov, H. J. Schött, A. P. Kabachenko, A. G. Popeko, and A. V. Yeremin, Nucl. Instr. and Meth. A **381**, 520 (1996).
[14] F. P. Heßberger, S. Antalic, B. Sulignano, D. Ackermann, S. Heinz, S. Hofmann, B. Kindler, J. Khuyagbaatar, I. Kojouharov, P. Kuusiniemi, M. Leino, B. Lommel, R. Mann, K. Nishio, A. G. Popeko, Š. Šáro, B. Streicher, J. Uusitalo, M. Venhard, and A. V. Yeremin, Eur. Phys. J. A **43**, 55 (2010).
[15] S. Hofmann, W. Faust, G. Münzenberg, W. Reisdorf, P. Armbruster, K. Güttner, and H. Ewald, Z. Phys. A **291**, 53 (1979).
[16] W. Reisdorf, Z. Phys. A **300**, 227 (1981).
[17] H. Kettunen, T. Enqvist, M. Leino, K. Eskola, P. T. Greenlees, K. Helariutta, P. Jones, R. Julin, S. Juutinen, H. Kankaanpää, H. Koivisto, P. Kuusiniemi, M. Muikku, P. Nieminen, P. Rahkila, and J. Uusitalo, Eur. Phys. J. A **16**, 457 (2003).
[18] A. N. Andreyev, S. Antalic, D. Ackermann, L. Bianco, S. Franchoo, S. Heinz, F. P. Heßberger, S. Hofmann, M. Huyse, I. Kojouharov, B. Kindler, B. Lommel, R. Mann, K. Nishio, R. D. Page, J. J. Ressler, P. Sapple, B. Streicher, Š. Šáro, B. Sulignano, J. Thomson, P. Van Duppen, and M. Venhart, Phys. Rev. C **79**, 064320 (2009).
[19] P. Van Duppen, P. Decrock, P. Dendooven, M. Huyse, G. Reusen, and J. Wauters, Nucl. Phys. A **529**, 268 (1991).
[20] M. Huyse, E. Coenen, K. Deneffe, P. Van Duppen, K. Heyde, and J. Van Maldeghem, Phys. Lett. B **201**, 293 (1988).
[21] R. B. Firestone, V. S. Shirley, S. Y. F. Chu, C. M. Baglin, and J. Zipkin, *Table of Isotopes*, CD-ROM Edition (John Wiley & Sons, New York, 1996).
[22] H. Kettunen, T. Enqvist, T. Grahn, P. T. Greenlees, P. Jones, R. Julin, S. Juutinen, A. Keenan, P. Kuusiniemi, M. Leino, A.-P. Leppänen, P. Nieminen, J. Pakarinen, P. Rahkila, and J. Uusitalo, Eur. Phys. J. A **17**, 537 (2003).
[23] K.-H. Schmidt, Z. Phys. A **316**, 19 (1984).
[24] H. De Witte, A. N. Andreyev, S. Dean, S. Franchoo, M. Huyse, O. Ivanov, U. Köster, W. Kurcewicz, J. Kurpeta, A. Plochocki, K. Van de Vel, J. Van de Walle, and P. Van Duppen, Eur. Phys. J. A **23**, 243 (2005).
[25] J. O. Rasmussen, Phys. Rev. **113**, 1593 (1959).
[26] M. Huyse, P. Decrock, P. Dendooven, G. Reusen, P. Van Duppen, and J. Wauters, Phys. Rev. C **46**, 1209 (1992).
[27] Z. Kalaninová (unpublished).
[28] S. Y. F. Chu, L. P. Ekström, and R. B. Firestone, The Lund/LBNL Nuclear Data Search (1999), http://nucleardata.nuclear.lu.se/nucleardata/toi/perchart.htm.
[29] M. B. Smith, R. Chapman, J. F. C. Cocks, O. Dorvaux, K. Helariutta, P. M. Jones, R. Julin, S. Juutinen, H. Kankaanpää, H. Kettunen, P. Kuusiniemi, Y. Le Coz, M. Leino, D. J. Middleton, M. Muikku, P. Nieminen, P. Rahkila, A. Savelius, and K.-M. Spohr, Eur. Phys. J. A **5**, 43 (1999).
[30] A. N. Andreyev, S. Antalic, M. Huyse, P. Van Duppen, D. Ackermann, L. Bianco, D. M. Cullen, I. G. Darby, S. Franchoo, S. Heinz, F. P. Heßberger, S. Hofmann, I. Kojouharov, B. Kindler, A.-P. Leppänen, B. Lommel, R. Mann, G. Münzenberg, J. Pakarinen, R. D. Page, J. J. Ressler, Š. Šáro, B. Streicher, B. Sulignano, J. Thomson, and R. Wyss, Phys. Rev. C **74**, 064303 (2006).
[31] H. Kettunen, J. Uusitalo, M. Leino, P. Jones, K. Eskola, P. T. Greenlees, K. Helariutta, R. Julin, S. Juutinen, H. Kankaanpää, P. Kuusiniemi, M. Muikku, P. Nieminen, and P. Rahkila, Phys. Rev. C **63**, 044315 (2001).
[32] J. Wauters, P. Dendooven, M. Huyse, G. Reusen, P. Van Duppen, P. Lievens, and The ISOLDE Collaboration, Phys. Rev. C **47**, 1447 (1993).
[33] F. Calaprice, G. T. Ewan, R.-D. von Dincklage, B. Jonson, O. C. Jonsson, and H. L. Ravn, Phys. Rev. C **30**, 1671 (1984).
[34] S. N. Liddick, R. Grzywacz, C. Mazzocchi, R. D. Page, K. P. Rykaczewski, J. C. Batchelder, C. R. Bingham, I. G. Darby, G. Drafta, C. Goodin, C. J. Gross, J. H. Hamilton, A. A. Hecht, J. K. Hwang, S. Ilyushkin, D. T. Joss, A. Korgul, W. Królas, K. Lagergren, K. Li, M. N. Tantawy, J. Thomson, and J. A. Winger, Phys. Rev. Lett. **97**, 082501 (2006).
[35] Z. Janas, C. Mazzocchi, L. Batist, A. Blazhev, M. Górska, M. Kavatsyuk, O. Kavatsyuk, R. Kirchner, A. Korgul, M. La Commara, K. Miernik, I. Mukha, A. Plochocki, E. Roeckl, and K. Schmidt, Eur. Phys. J. A **23**, 197 (2005).
[36] D. Schardt, T. Batsch, R. Kirchner, O. Klepper, W. Kurcewicz, E. Roeckl, and P. Tidemand-Petersson, Nucl. Phys. A **368**, 153 (1981).